Electronic Supplementary Material (ESI) for Journal of Materials Chemistry C.

Supplementary Information: SIn2Te/TeIn2Se: a type-II heterojunction as water-splitting photocatalyst with high solar energy harvesting

Peishun Shan[1], Chunxiao Zhang[1,2], Mengshi Zhou[1], Chaoyu He[1,2], Tao Ouyang[1,2], Jin Li[1,2], Chao Tang[1] and Jianxin Zhong[1]

[1]Hunan Key Laboratory for Micro-Nano Energy Materials and Devices, Laboratory for Quantum Engineering and Micro-NanoEnergy Technology, School of Physics and Optoelectronics, Xiangtan University, Hunan 411105, People's Republic of China

[2]Department of optoelectronic information science and technology, School of Physics and Optoelectronics, Xiangtan University, Hunan 411105, People's Republic of China

* Corresponding authors. Tel +86 731 58292195 E-mail: zhangchunxiao@xtu.edu.cn (C. Zhang)
** Corresponding authors. Tel +86 731 58292437 E-mail:tang_chao@xtu.edu.cn (C. Tang)

Table S1 In-Plane lattice constant (a) and bond lengths of M-M, M-X, M-Te for M2XTe(in Å), bandgap E_g(eV).

material	a	M-M	M-X	M-Te	E_g(PBE)	E_g(HSE06)
SeGa2Te	3.985	2.471	2.552	2.665	1.22	1.92
SGa2Te	3.900	2.472	2.449	2.643	0.90	1.57
SeIn2Te	4.244	2.814	2.729	2.857	1.15	1.80
SIn2Te	4.166	2.815	2.624	2.839	0.90	1.53

Table S2 The calculated binding energy(E_b) of the M2XTe heterostructures with different stacking.

System (Lattice mismatch)	Stacking （types）	E_b （eV）	System (Lattice mismatch)	Stacking （types）	E_b （eV）
SeIn2Te/SeGa2Te	AA	-0.1023	SIn2Te/SeIn2Te	AA	-0.1636
(6.10%)	AB-Te-Ga	-0.2023	(1.88%)	AB-Te-In	-0.2838
	AB-In-Se	-0.2136		AB-In-Se	-0.2876
TeIn2Se/TeGa2Se	AA	-0.1049	TeIn2S/SeIn2Te	AA	-0.1266
	AB-Se-Ga	-0.2162		AB-S-In	-0.2418
	AB-In-Te	-0.2191		AB-In-Se	-0.2483
TeIn2Se/SeGa2Te	AA	-0.0824	TeIn2S/TeIn2Se	AA	-0.1469
	AB-In-Se	-0.1875		AB-S-In	-0.2659
	AB-Se-Ga	-0.1817		AB-In-Te	-0.2650
SeIn2Te/TeGa2Se	AA	-0.1225	SIn2Te/TeIn2Se	AA	-0.1809
	AB-In-Te	-0.2518		AB-Te-In	-0.3161
	AB-Te-Ga	-0.2429		AB-In-Te	-0.3173
SGa2Te/SeGa2Te	AA	-0.1327	SIn2Te/SeGa2Te	AA	-0.1296
(2.13%)	AB-Te-Ga	-0.2269	(4.32%)	AB-Te-Ga	-0.2268
	AB-Ga-Se	-0.2324		AB-In-Se	-0.2392
TeGa2S/SeGa2Te	AA	-0.0949	TeIn2S/SeGa2Te	AA	-0.0932
	AB-S-Ga	-0.1736		AB-S-Ga	-0.1874
	AB-Ga-Se	-0.1765		AB-In-Se	-0.1970
TeGa2S/TeGa2Se	AA	-0.1159	TeIn2S/TeGa2Se	AA	-0.1153
	AB-S-Ga	-0.2035		AB-S-Ga	-0.2200
	AB-Ga-Te	-0.1992		AB-In-Te	-0.2239
SGa2Te/TeGa2Se	AA	-0.1523	SIn2Te/TeGa2Se	AA	-0.1513
	AB-Te-Ga	-0.2664		AB-Te-Ga	-0.2690
	AB-Ga-Te	-0.2672		AB-In-Te	-0.2777
SGa2Te/SeIn2Te	AA	-0.0238	SIn2Te/SGa2Te	AA	-0.0490
(8.01%)	AB-Te-In	-0.1342	(6.25%)	AB-Te-Ga	-0.1329
	AB-Ga-Se	-0.1318		AB-In-S	-0.1434
TeGa2S/SeIn2Te	AA	-0.0176	TeIn2S/SGa2Te	AA	-0.0131
	AB-S-In	-0.0723		AB-S-Ga	-0.0995

	AB-Ga-Se	-0.0723		AB-In-S	-0.1031
TeGa2S/TeIn2Se	AA	-0.0018	TeIn2S/TeGa2S	AA	-0.0518
	AB-S-In	-0.0987		AB-S-Ga	-0.1543
	AB-Ga-Te	-0.0891		AB-In-Te	-0.1549
SGa2Te/TeIn2Se	AA	-0.0400	SIn2Te/TeGa2S	AA	-0.0887
	AB-Te-In	-0.1696		AB-Te-Ga	-0.2055
	AB-Ga-Te	-0.1617		AB-In-Te	-0.2140

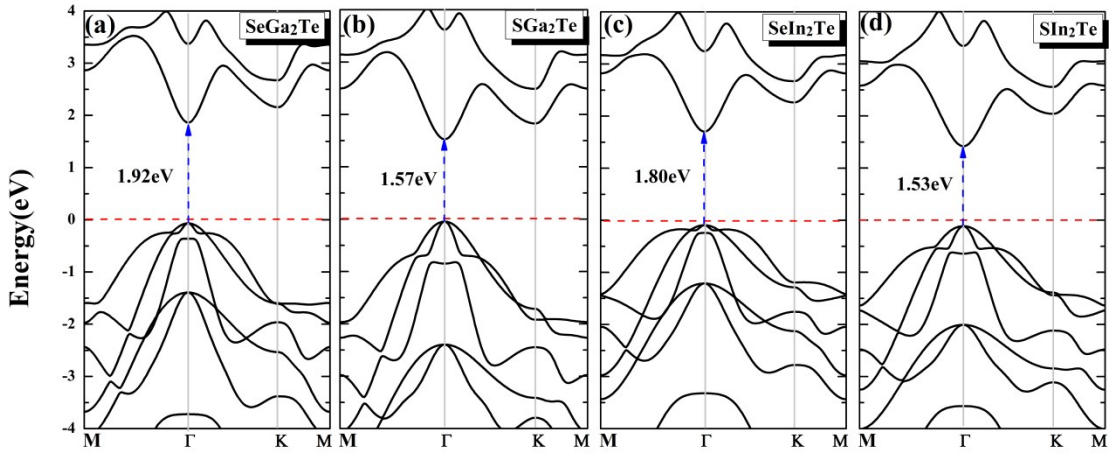

Fig. S1 Band structure of single-layer (a) SeGa2Te, (b) SGa2Te, (c) SeIn2Te, (d) SIn2Te in HSE06.

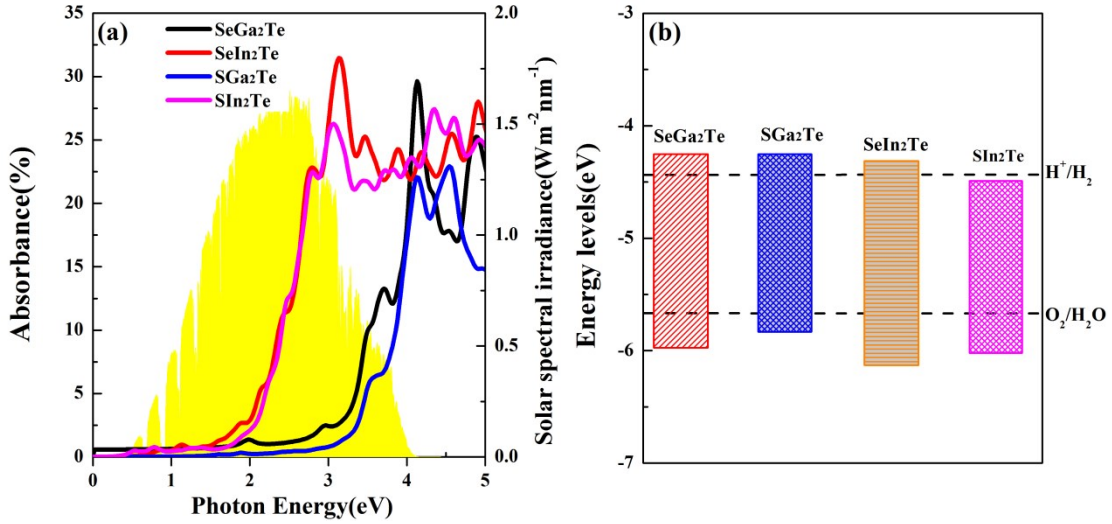

Fig. S2 (a) Optical absorbance A(E) of Janus SeGa2Te, SeIn2Te, SGa2Te and SIn2Te, respectively. (b) The band edge alignment of the redox potential of Janus SeGa2Te, SeIn2Te, SGa2Te and SIn2Te relative to water calculated by the HSE06 method. The

black dotted line indicates the redox potential of water. The reference air-mass 1.5-solar-spectral irradiance is plotted in yellow.

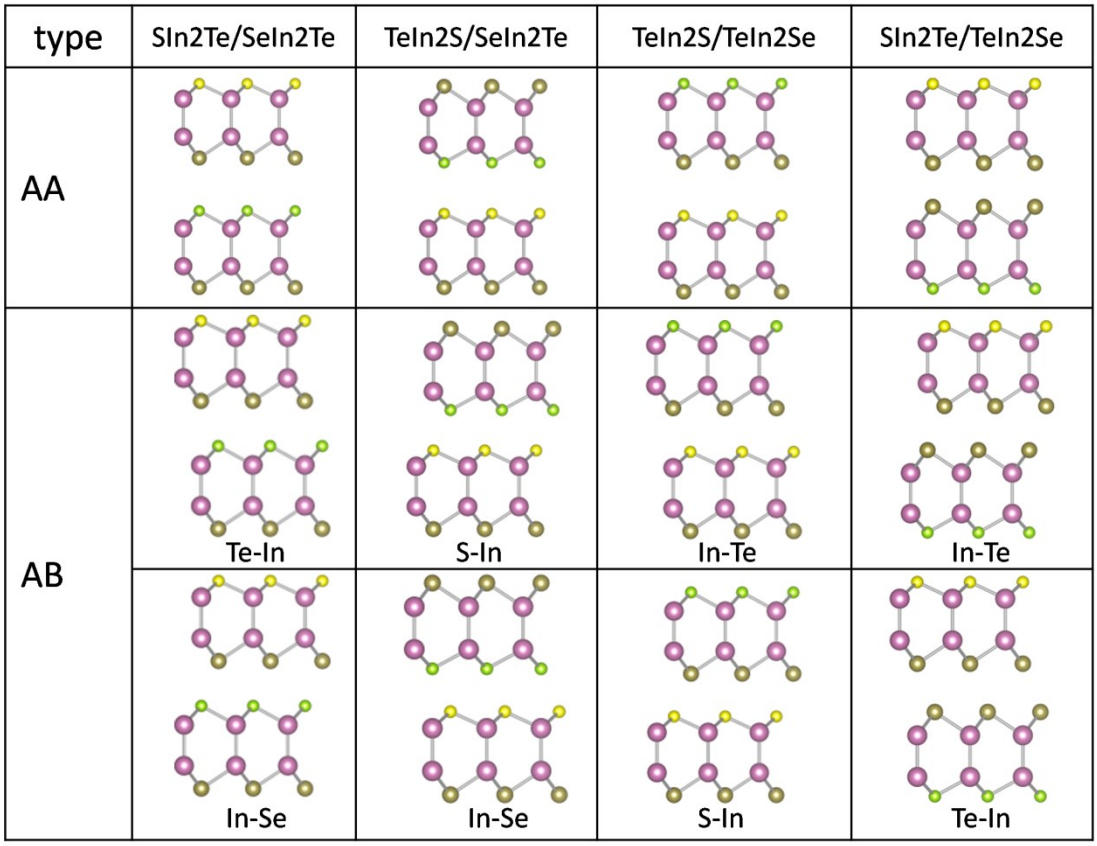

Fig. S3 Various stacking configurations of SIn2Te/SeIn2Te heterojunction. In the naming format "AB-a1-a2", the a1 and a2 stand for the opposite atoms at the interface. For example, the AB-In-Te means that the In atom from SIn2Te is directly above the Te atom from SeIn2Te in AB stacking SIn2Te/SeIn2Te. The XM2Te/XM2Te and XM2Te/TeM2X follow this stacking rule.

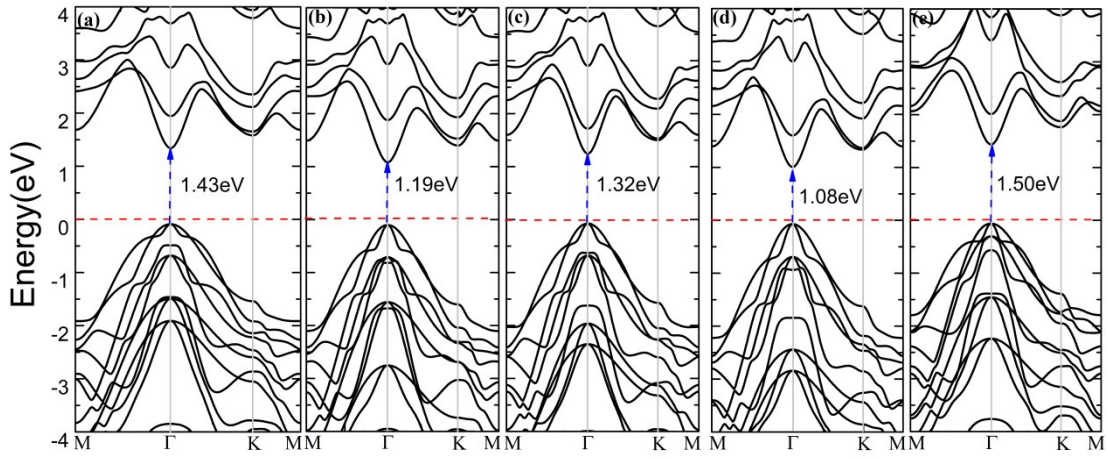

Fig. S4 Band structures of vdW heterojunctions in their most stable stacking. (a) SeIn2Te/TeGa2Se, (b) SGa2Te/TeIn2Se, (c) SIn2Te/TeGa2Se, (d) SIn2Te/TeGa2S, (e) SIn2Te/TeIn2Se

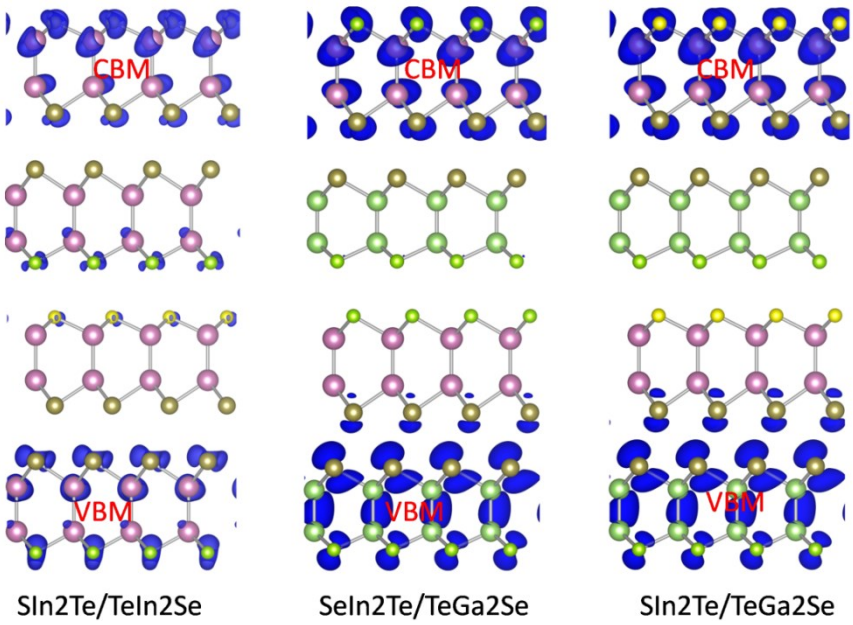

Fig. S5 The band-decomposed charge density of the CBM and VBM of SIn2Te/TeIn2Se, SeIn2Te/TeGa2Se and SIn2Te/TeGa2Se, respectively.(The isosurface is 0.005 $|e|Å^3$).

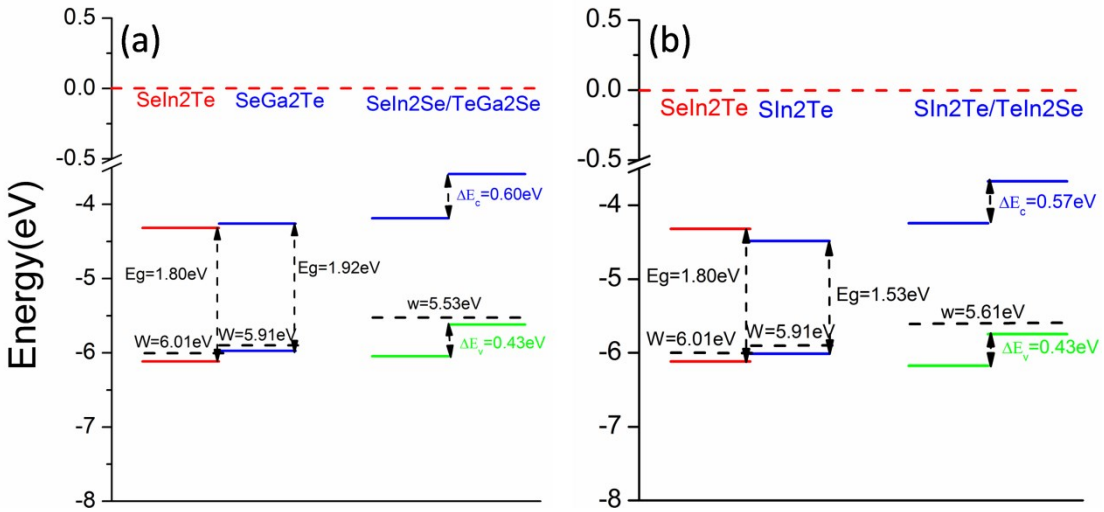

Fig. S6 The band alignment of (a) SeIn2Te/TeGa2Se and (b) SIn2Te/TeIn2Se heterojunctions.

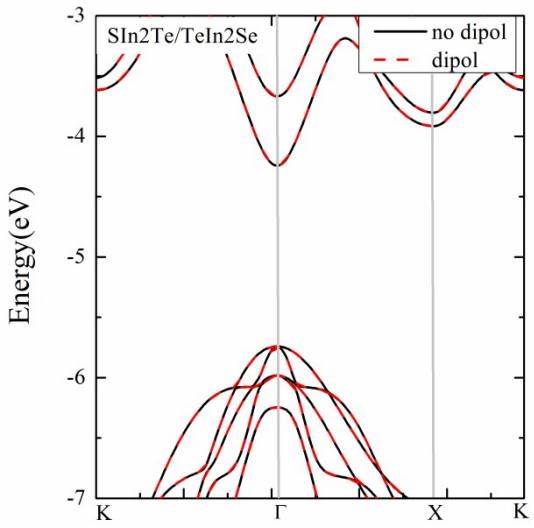

Fig. S7 The band structure of SIn2Te/TeIn2Se heterojunction relative to vacuum energy level. (red and black lines with and without dipole correction, respectively)

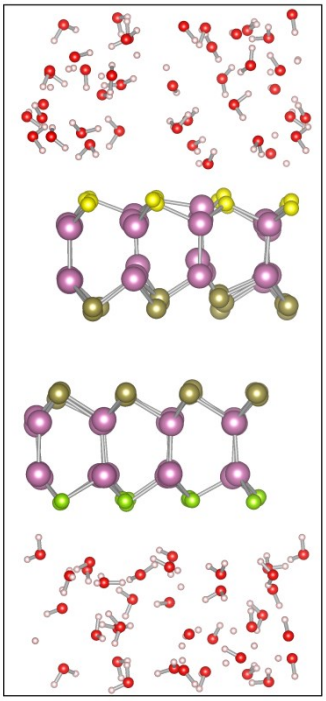

Fig. S8 Snapshot structure of SIn2Te/TeIn2Se heterojunction in liquid water after stabilizing at 500K for 6ps. (The simulation was carried out by placing the SIn2Te/TeIn2Se heterojunction in liquid water with a density of 1g/cm^3)

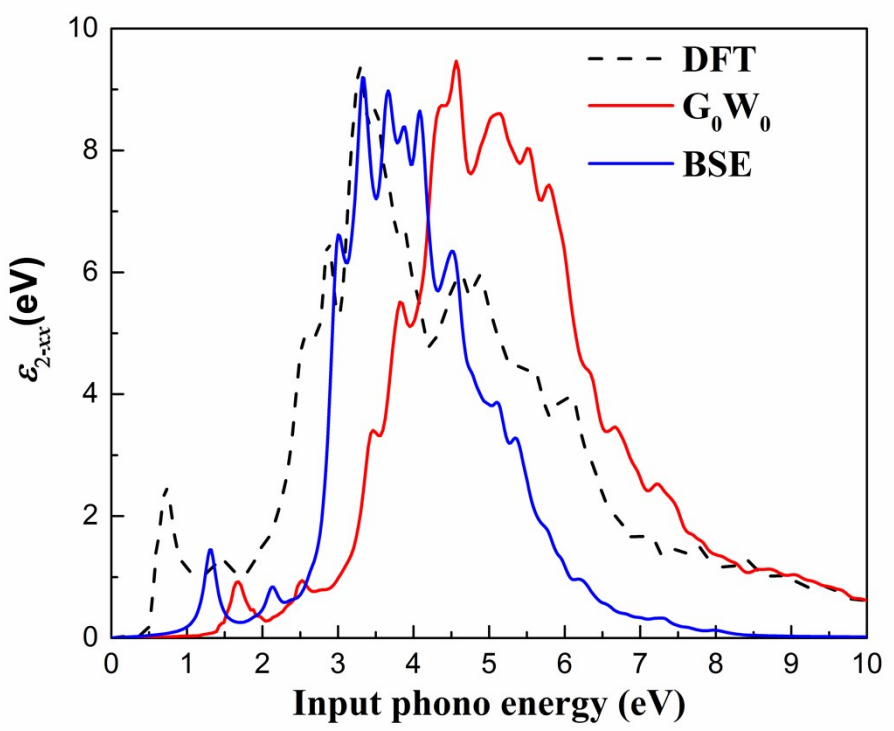

Fig. S9 Imaginary part of dielectric function of SIn2Te/TeIn2Se heterojunction

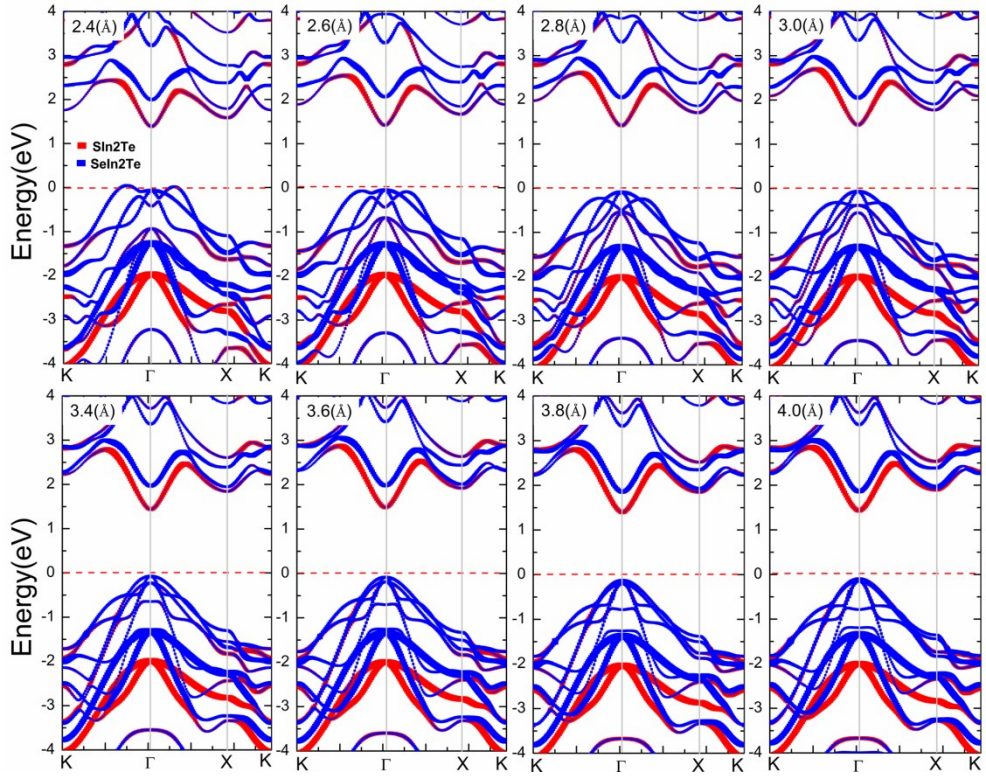

Fig. S10 Projection band structure of SIn2Te/TeIn2Se as interlayer distance varies from 2.40Å to 4.00Å and the spacing is 0.2Å.

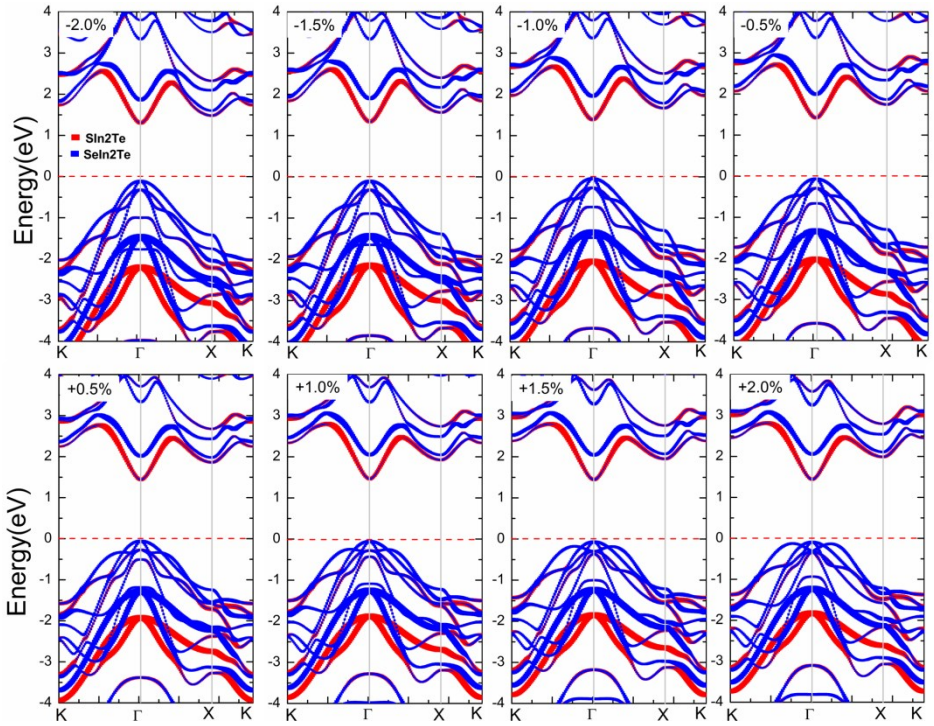

Fig. S11 Projection band structure of the SIn2Te/TeIn2Se as biaxial strain increases from -2.0% to 2.0% with 0.5% interval.

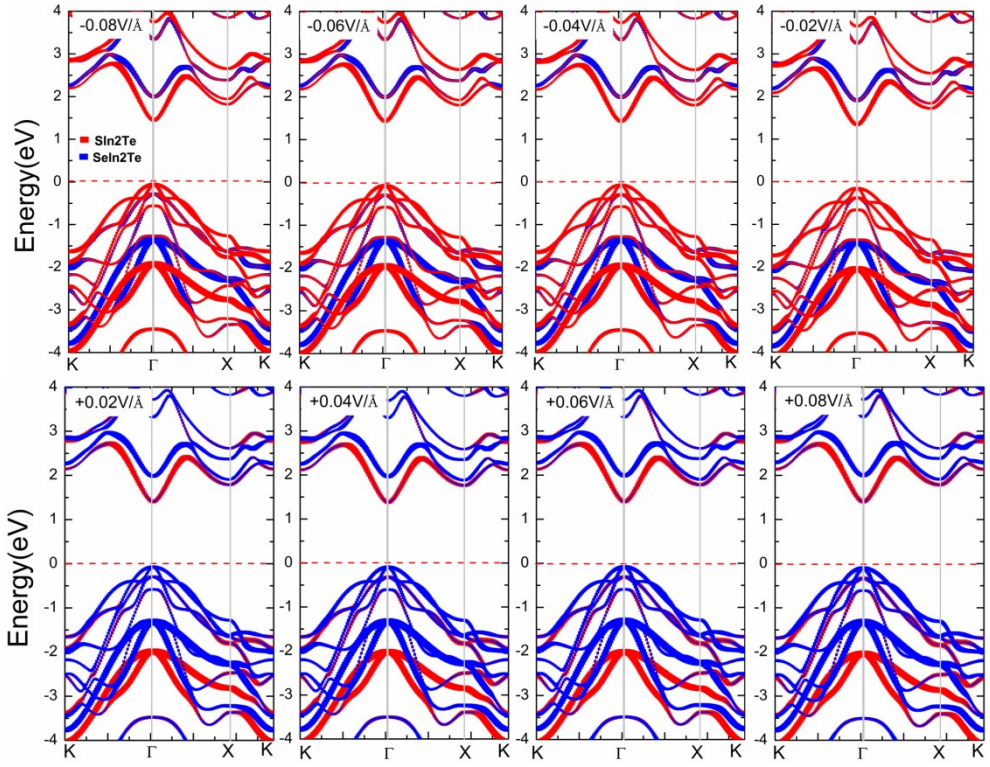

Fig. S12 Projection band structure with vertical E-field from -0.08V/Å to +0.08V/Å with an interval of 0.02V/Å.

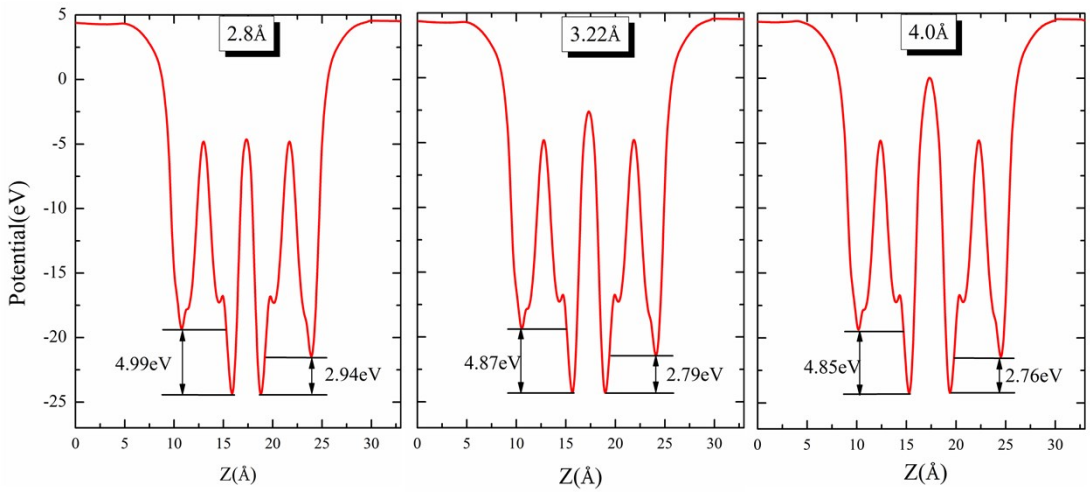

Fig. S13 Plane-averaged potential $\overline{V}$ (red line) of SIn2Te/TeIn2Se vdW under specific interlayer distance.

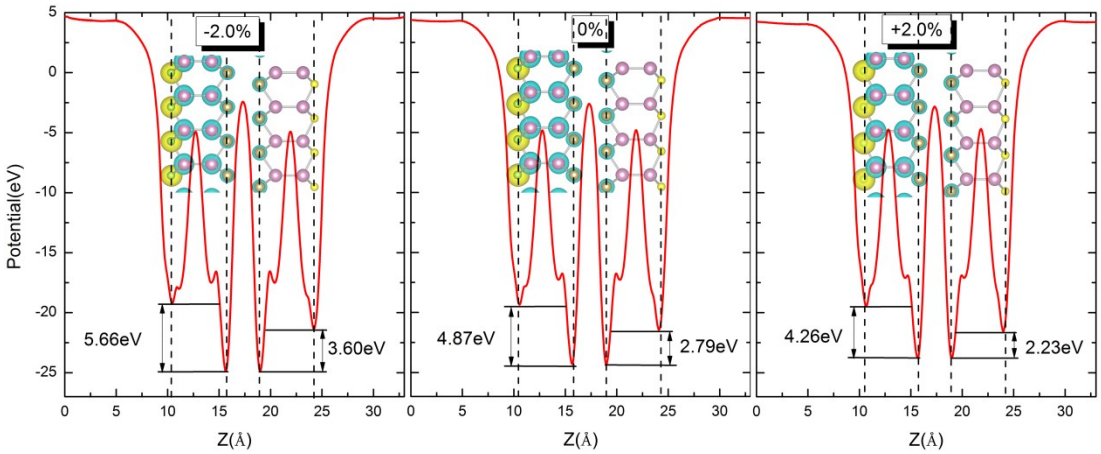

Fig. S14 Plane-averaged potential $\overline{V}$ (red line) of SIn2Te/TeIn2Se vdW under specific in-plane strain. The inset represents the 3Disosurface of the differential electron density for the SIn2Te/TeIn2Se.The yellow and blue regions represent electron accumulation and depletion, respectively. The isosurface is 0.03 |e|Å^3

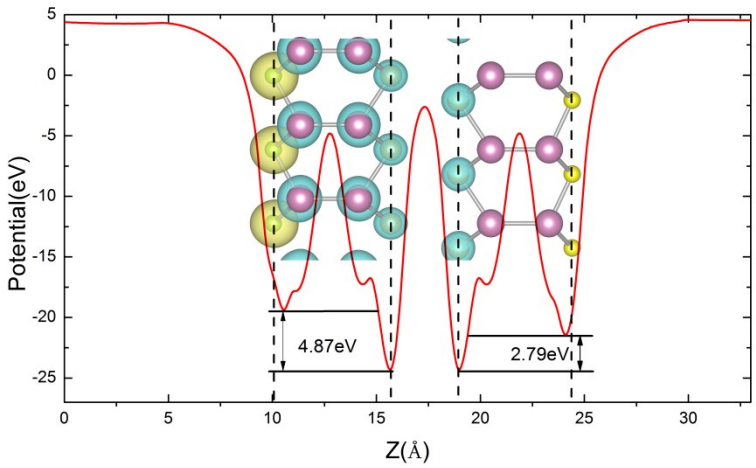

Fig. S15 Plane-averaged potential $\overline{V}$ (red line) for the SIn2Te/TeIn2Se. The inset represents the 3D isosurface of the differential electron density for the SIn2Te/TeIn2Se. The yellow and blue regions represent electron accumulation and depletion, respectively. The isosurface is 0.03 |e|/Å^3

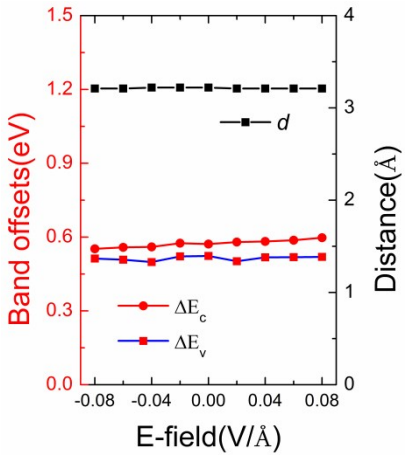

Fig. S16 Evolution of interlayer distance *d*(**Å**) and band offsets of SIn2Te/TeIn2Se with increasing of the E-field.

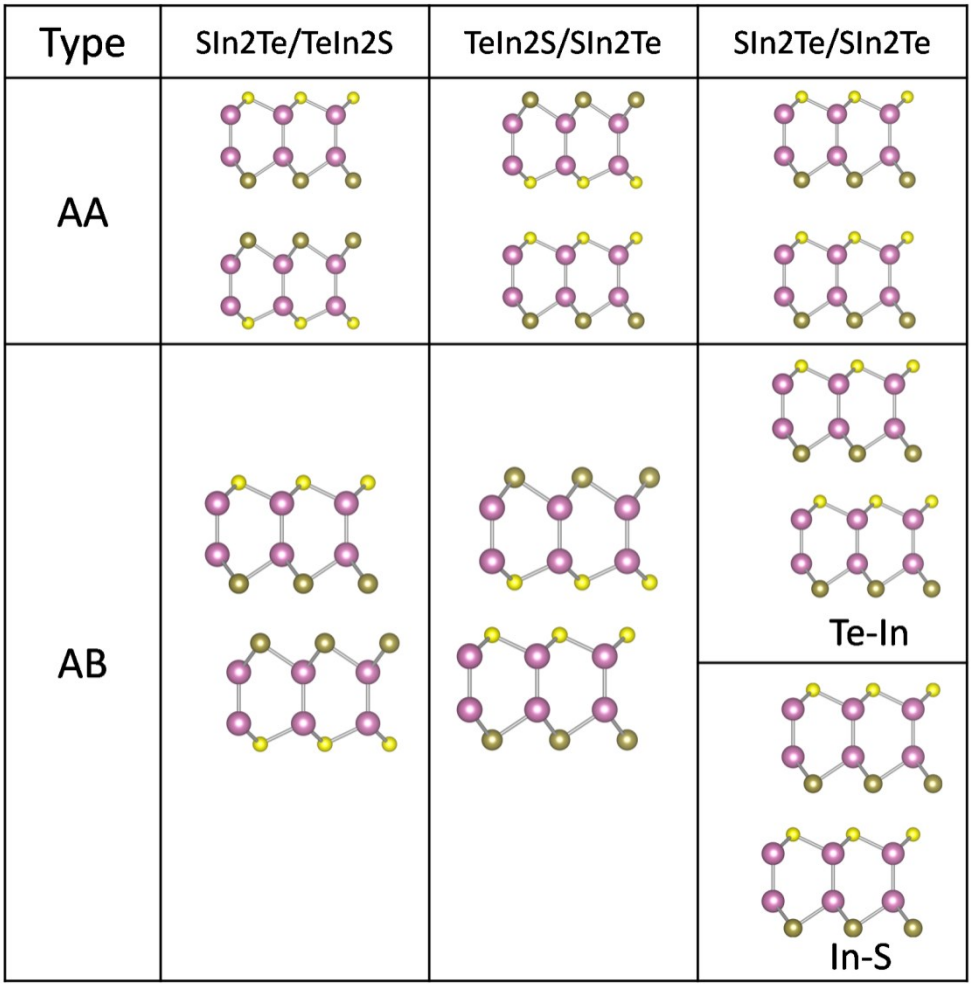

Fig. S15 Various stacking configurations of SIn2Te bilayer heterojunction.

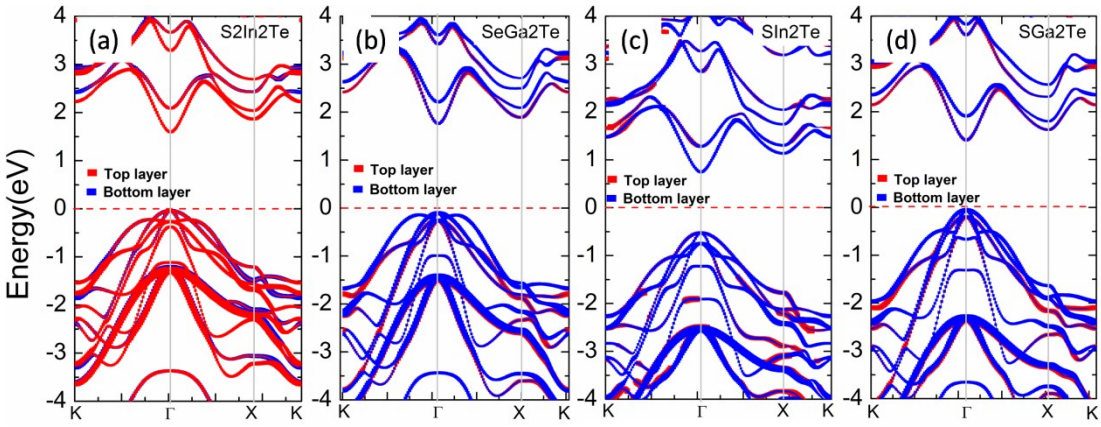

Fig. S16 Projection band structures of the Janus bilayers (a) SeIn2Te/TeIn2Se, (b) SeGa2Te/TeGa2Se, (c) SIn2Te/TeIn2S and (d) SGa2Te/TeGa2S.

Table S3 Binding energy (E_b) of the different stacking configurations for the M2XTe bilayers heterojunction.

System（Bilayers）	Stacking（type）	E_b（eV）	System（Bilayers）	Stacking（sype）	E_b（eV）
TeGa2Se/TeGa2Te	AA	-0.1594	TeIn2Se/TeIn2Se	AA	-0.1851
	AB-Se-Ga	-0.2602		AB-Se-In	-0.3134
	AB-Te-Ga	-0.2553		AB-Te-In	-0.3106
SeGa2Te/TeGa2Se	AA	-0.1789	SeIn2Te/TeIn2Se	AA	-0.2021
	AB	-0.2940		AB	-0.3388
TeGa2Se/SeGa2Te	AA	-0.1390	TeIn2Se/SeIn2Te	AA	-0.1652
	AB	-0.2273		AB	-0.2883
TeIn2S/TeIn2S	AA	-0.1418	TeGa2S/TeGa2S	AA	-0.1163
	AB-S-In	-0.2572		AB-S-Ga	-0.2039
	AB-Te-In	-0.2536		AB-Te-Ga	-0.1988
SIn2Te/TeIn2Te	AA	-0.1754	SGa2Te/TeGa2S	AA	-0.1540
	AB	-0.3101		AB	-0.2680
TeIn2S/SIn2Te	AA	-0.1039	TeGa2S/SGa2Te	AA	-0.0809
	AB	-0.2202		AB	-0.1537

Table S4 In-Plane lattice constant a, Interlayer d(Å), bandgap Eg (eV), band alignment, band-gap type.

Material（Bilayers）	a（Å）	d (Å)	Eg(PBE) (eV)	Eg(HSE06) (eV)	Band alignment	Type
SeIn2Te/TeIn2Se	4.099	3.21	0.94	1.63	Type-I	D
SeGa2Te/TeGa2Se	3.911	3.36	1.11	1.86	Type-I	D
SIn2Te/TeIn2S	4.030	3.22	0.60	1.27	Type-I	D
SGa2Te/TeGa2S	3.837	3.37	0.74	1.46	Type-I	D